Mechanism of Action of Thrombin on Fibrinogen: NMR Evidence for a β-Bend at or near Fibrinogen Aα Gly(P_5)-Gly(P_4)†

H. C. Marsh, Jr.,‡ Y. C. Meinwald, S. Lee, R. A. Martinelli, and H. A. Scheraga*
Baker Laboratory of Chemistry, Cornell University, Ithaca, New York 14853
Received August 30, 1984

ABSTRACT: The following synthetic linear Aα fibrinogen-like peptides were studied by NMR spectroscopy in aqueous solution: Ac-Asp(P_{10})-Phe(P_9)-Leu-Ala-Glu-Gly(P_5)-Gly(P_4)-Gly(P_3)-Val-Arg(P_1)-Gly-(P_1')-Pro-Arg(P_3')-Val-$NHCH_3$ (F-8), Ac-Phe-Leu-Ala-Glu-Gly-Gly(P_4)-Gly(P_3)-Val-Arg-Gly-Pro-$NHCH_3$ (F-6), Ac-Leu-Ala-Glu-Gly-Gly(P_4)-Gly(P_3)-Val-Arg-Gly-Pro-$NHCH_3$ (F-7), and Ac-Gly-Gly(P_4)-Gly-(P_3)-Val-Arg-Gly-Pro-$NHCH_3$ (F-9). The temperature dependence of the amide proton chemical shift is smaller by approximately 22% for the Gly(P_3) amide proton in F-9, F-6, and F-8 and is similarly smaller for the Gly(P_4) amide proton in F-6 and F-8, but not F-9, relative to the other amide protons in these peptides. The exchange rates with solvent water for the Gly(P_3) amide proton in each of these four peptides were determined by solvent spin saturation transfer experiments. The exchange rate constant for the Gly(P_3) amide proton of F-8 was half that of the rate constant determined for this proton in F-9, F-7, and F-6. In conjunction with previously reported data for the rate of hydrolysis of the Arg(P_1)–Gly(P_1') bond by thrombin, these results suggest that there is a β-bend at Gly(P_5)-Gly(P_4), possibly stabilized by salt links between Asp(P_{10}) and Arg(P_3') and between phosphorylated Ser(P_{14}) and Arg(P_7'), which brings Phe(P_9) close to the hydrolyzable Arg–Gly bonds. This explanation accounts for the importance of Phe(P_9) for thrombin action, for diminished activity of several abnormal fibrinogens that have amino acid substitutions at positions P_{10} and P_3', and for the enhanced activity of fibrinogen with Ser(P_{14}) phosphorylated.

From the observation that the amino acid sequence in a portion of the fibrinogens of many species is strongly conserved, Blombäck (1967) had suggested that Phe at position P_9[1] of the Aα chain of fibrinogen is essential for normal thrombin action in which an Arg–Gly bond of the Aα chain is hydrolyzed. This suggestion was confirmed by subsequent kinetic experiments involving a series of synthetic peptide substrates (Van Nispen et al., 1977; Meinwald et al., 1980; Marsh et al., 1982). To explain the large effect of a single amino acid residue nine residues distant in the linear sequence from the site of enzyme action, it was proposed that the intervening residues might accommodate a feature such as a β-bend that would allow the Phe at position P_9 to be brought into close spatial proximity to the Arg–Gly bond that is hydrolyzed. The existence of a β-bend is supported by the high reactivity of D-phenylalanylvalylarginine *p*-nitroanilide (but not the corresponding L-Phe compound) toward thrombin (Claeson et al., 1977) and by NMR observations (Rae & Scheraga, 1979) that indicate that the D-Phe residue is folded back over the Val residue but that this arrangement is not found in the L-Phe peptide.

While peptides containing Phe at P_9 (but not Asp at P_{10}) are substantially better substrates than those lacking this residue, they are poorer substrates of thrombin than even CNBr Aα, primarily because of differences in binding affinities reflected in the values of the Michaelis–Menten parameter K_M. On the basis of immunochemical studies, Nagy et al. (1982) concluded that it is possible that these substrates contain all the residues that interact directly at the active site of thrombin yet lack residues that provide the long-range interactions necessary to stabilize the native conformation required for normal binding at the active site.

Direct involvement of Asp at P_{10} can be inferred from the abnormal rate of release of fibrinopeptide A from fibrinogen Lille, in which Asn replaces Asp at P_{10} (Morris et al., 1981). Furthermore, an acid residue (Asp or Glu) is present at position P_{10} in most fibrinogen species (Dayoff, 1972, 1973, 1976). The importance of Asp(P_{10}) in thrombin–fibrinogen interactions was established by comparing the Michaelis–Menten parameters for the hydrolysis of the Arg(P_1)–Gly(P_1') bond in peptide F-8 (defined in Table I) to those of a series of similar fibrinogen-like peptides lacking Asp(P_{10}) (Marsh et al., 1983).

It has been suggested (Morris et al., 1981; Nagy et al., 1982; Marsh et al., 1983) that a salt link between Asp at position P_{10} and Arg at position P_3' stabilizes an intervening β-bend, thus providing the proper orientation of Phe(P_9) with respect to the active site of thrombin. The absence of such long-range interactions would explain the delayed release of fibrinopeptide A from fibrinogen Lille and from fibrinogen Munich in which Asn replaces Arg at P_3' (Henschen et al., 1981). Alternatively, Asp(P_{10}) may possibly interact directly with the thrombin molecule itself.

† This work was supported by research grants from the National Institute of General Medical Sciences (GM-24893) and from the National Heart, Lung and Blood Institute (HL-30616). It was carried out with the 600-MHz NMR spectrometer at Carnegie-Mellon University (NIH-RR-00292) and the Brüker WM 300 NMR spectrometer at Cornell University (NSF-CHE-79-04825). This is paper 15 in a series. Hanna et al. (1984) is paper 14 of this series.

‡ National Institutes of Health Postdoctoral Fellow, 1980–1983. Present address: Abbott Laboratories, North Chicago, IL 60064.

[1] Abbreviations: Ac, acetyl; Boc, *tert*-butyloxycarbonyl; DCC, *N*,*N*′-dicyclohexylcarbodiimide; HOBt, 1-hydroxybenzotriazole; Me, methyl; CNBr Aα, the N-terminal CNBr fragment of the Aα chain of fibrinogen; TLC, thin-layer chromatography; NMR, nuclear magnetic resonance; pH*, pH meter reading in aqueous solutions containing D_2O; SST, solvent spin saturation transfer. The positions of residues in peptide substrates are described by the nomenclature of Schechter & Berger (1967) wherein residues on the N-terminal side of the Arg–Gly bond are designated as P_1, P_2, etc. and those on the C-terminal side are designated as P_1', P_2', etc. (see Table I). The amino acid sequences of peptides F-3 and F-4 are given in Table I of Marsh et al. (1983) and those of peptides F-5 to F-9 are given in Table I of this paper.

0006-2960/85/0424-2806$01.50/0

Table I: Amide Proton Chemical Shifts[a] (ppm) at 300 K and 300 MHz, or Room Temperature and 600 MHz

peptide		P_{10}	P_9	P_8	P_7	P_6	P_5	P_4	P_3	P_2	P_1	P_1'	P_2'	P_3'	P_4'	P_5'
F-8	Ac	Asp	Phe	Leu	Ala	Glu	Gly	Gly	Gly	Val	Arg	Gly	Pro	Arg	Val	NHMe
							8.47	8.33	8.29	8.04		NR[b]				8.08
F-5		Ac	Phe	Leu	Ala	Glu	Gly	Gly	Gly	Val	Arg	Gly	Pro	Arg	Val	NHMe
							8.47	8.34	8.30	8.05		8.25				8.08
F-6		Ac	Phe	Leu	Ala	Glu	Gly	Gly	Gly	Val	Arg	Gly	Pro	NHMe		
							8.50	8.34	8.31	8.07		8.27		7.99		
F-7			Ac	Leu	Ala	Glu	Gly	Gly	Gly	Val	Arg	Gly	Pro	NHMe		
							8.49	8.35	8.32	8.07		NR		7.98		
F-9						Ac	Gly	Gly	Gly	Val	Arg	Gly	Pro	NHMe		
							8.49	8.37	8.35	8.07	8.50	8.27		7.98		

[a] Slight differences between the values reported here and those in Figure 2 arise because the chemical shifts were referenced to a broad water peak. Data for F-5, F-6, and F-7 were obtained at 600 MHz; those for F-6, F-7, F-8, and F-9 were also obtained at 300 MHz. All data in this table are for the centers of multiplets. [b] Not resolved.

To obtain direct evidence for the proposed Asp(P_{10}) to Arg(P_3') salt link and intervening β-bend, an NMR study of the peptides prepared for the kinetic experiments was undertaken. In aqueous solution, short, linear peptides such as those considered here generally exist as an ensemble of many conformational states of similar free energy; i.e., they do not adopt a single native, low-energy form as do their larger protein counterparts. The NMR spectra from solutions of these peptides reflect averages over the various conformations, and at best, only subtle differences in the NMR spectra between the various peptides are observable. In the past, attempts to demonstrate conformational features in small, linear peptides in aqueous solution have met with little success, except in favorable cases where specific local interactions lead to a dominance of one conformation in the ensemble (Montelione et al., 1984). NMR evidence for conformational details in small peptides, in general, has been obtained by use of nonaqueous solvents such as Me_2SO and/or use of cyclized peptides whose conformational freedom is greatly restricted. The linear peptides studied here exhibit measurable, though small differences in NMR behavior, which may reflect stronger conformational tendencies in the native protein.

Materials and Methods

All of the amino acids (except glycine) were of the L configuration. Boc-Arg(NO_2)-OH was purchased from Vega Biochem. Co., Ac-Gly-OH was from Sigma Chemical Co., and DCC and HOBt were from Aldrich Chemical Co. We thank Dr. G. T. Taylor for preparing the H-[$^2H_2$]Gly-OH. CM-52 was obtained from Whatman Ltd.

The purity of the amino acid derivatives and peptides was checked routinely by TLC on Merck silica gel plates (F-254, 0.25 mm) in the following solvent systems: (a) chloroform–methanol, 5:1; (b) chloroform–methanol–acetic acid, 95:20:3; (c) 1-butanol–acetic acid–pyridine–water, 4:1:1:2; (d) 2-propanol–formic acid–water, 20:1:5.

Synthetic Methods. Three different preprations of F-6 (defined in Table I) were synthesized with perdeuterated glycine (H-[$^2H_2$]Gly-OH) in positions P_4, P_3, and P_1', respectively, by a procedure reported by Meinwald et al. (1980) with a slight modification. A new route for the C-terminal hexapeptide H-Gly-Gly-Val-Arg-Gly-Pro-$NHCH_3$ (VIII) was developed in order to incorporate the H-[$^2H_2$]Gly-OH in the three different positions in a most efficient way. The new synthetic scheme is presented in Figure 1.

Heptapeptide fragment Ac-Gly-[$^2H_2$]Gly-Gly-Val-Arg-Gly-Pro-$NHCH_3$ (F-9) was prepared by coupling Ac-Gly-OH with H-[$^2H_2$]Gly-Gly-Val-Arg-Gly-Pro-$NHCH_3$ by the DCC/HOBt method. The detailed experimental procedure and the properties of the new intermediates are presented in the supplementary material (see paragraph at end of paper regarding supplementary material). The syntheses of the other peptides have been described previously (Van Nispen et al., 1977; Meinwald et al., 1980; Marsh et al., 1982, 1983).

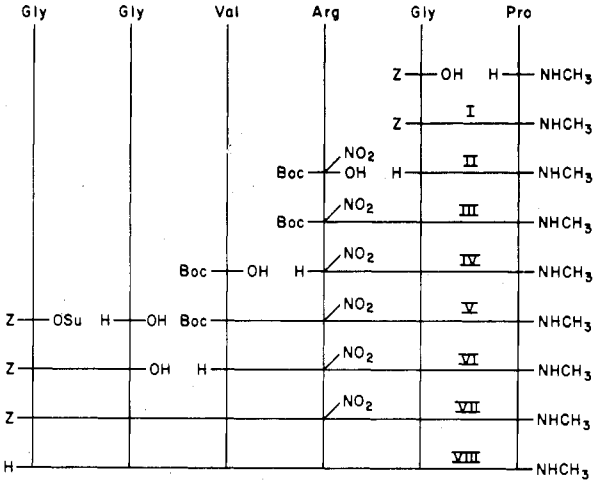

FIGURE 1: Schematic representation of the synthesis of the hexapeptide H-Gly-Gly-Val-Arg-Gly-Pro-$NHCH_3$.

NMR Measurements. For resonance assignments, proton NMR spectra of peptides F-3 to F-7 (10–20 mg/mL in H_2O or D_2O) were obtained at room temperature on the 600-MHz spectrometer at Carnegie-Mellon University operating in the correlation mode. Difference spectra, obtained by decoupling on- and off-resonance of the peak of interest, established the spin–spin connectivities. Resonance assignments for peptides F-8 and F-9 were obtained in a similar manner on the Bruker WM300 spectrometer at Cornell University. Two-dimensional NMR spectra (two-dimensional *J*-resolved and SECSY, Bruker programs) provided resolution of overlapping multiplets and established many spin–spin connectivities in peptide F-8 at 300 MHz. Since peptide F-8 precipitates at low pH, it was not possible to obtain pH-dependent NMR spectra (or potentiometric titration data) in order to detect the putative salt link in this peptide.

Temperature Dependence of Amide Proton Chemical Shift. Aqueous solutions of peptides F-6 (50 mM, pH* 4.9), F-8 (30 mM, pH* 4.5), and F-9 (32 mM, pH* 4.8) were used to obtain data on the temperature dependence of the chemical shifts of the amide protons. Each solution contained 7% D_2O for a lock signal. The spectra were recorded on a Bruker WM300 spectrometer using a Redfield (2–1–4) tailored excitation pulse (Redfield et al., 1975); no base-line corrections were applied. Temperatures represent the nominal values on the variable-temperature control unit.

Chemical shifts were referenced with respect to the water (HOD) resonance, defined as 4.80 ppm at 300 K at pH* 4.9, 4.5, and 4.8 for F-6, F-8, and F-9, respectively; spectra at the

same pH*s but at other temperatures were referenced internally with respect to a nonexchanging proton that had previously been referenced with respect to HOD at 300 K. Spectra of F-6 and F-8 were referenced to the phenyl ring δ-proton of Phe(P_9). Spectra of F-9 were referenced to the upfield peak of the methyl proton doublet of *trans*-proline *N*-methylamide. The temperature dependence of the chemical shift of each peak was found to be linear. For F-6 and F-9, the curves for all peaks of a particular multiplet were found to have the same slopes, and the data are presented only for the centers of the multiplets. For F-8, the curves are presented for each peak of a multiplet; however, for clarity, only the centers of the multiplets for the Gly(P_3) and Gly(P_4) amides are presented.

Amide Proton Exchange Rate. All determinations of amide proton exchange rates were made on a Bruker WM300 spectrometer using a Redfield 2–1–4 observation pulse. Peptide concentrations ranged from 19 to 23 mM in H_2O, in 5-mm NMR tubes with a coaxial insert containing D_2O for a lock signal. The sample pH was adjusted with submicroliter quantities of dilute HCl or NaOH. The pH of the sample was measured directly in the NMR tube with an Ingold electrode and a Radiometer PHM82 standard pH meter immediately following each NMR experiment. All determinations of exchange rates were made at the nominal value of 300 K on the temperature control unit. The determination of exchange rates consisted of two experiments: a steady-state solvent spin saturation transfer experiment and a saturation–recovery relaxation determination. The theoretical basis for the measurements has been presented elsewhere (Campbell et al., 1977, 1978; Krishna et al., 1979, 1980).

Solvent Spin Saturation Transfer (SST) Experiments. Prior to each SST experiment, a saturation (>95%) of the solvent water peak was demonstrated using a normal short observation pulse with all other parameters identical with those used in the actual experiments. Quantitative estimates of solvent saturation transfer were obtained by measuring the peak intensities of the resonance of interest in the presence (I_{sat}) and absence (I_0) of solvent water saturation. The fractional decrease in peak intensity, η, was then computed as $\eta = (I_0 - I_{sat})/I_0$.

Saturation–Recovery Relaxation Experiments. The amide proton resonance of interest was saturated with the decoupler, and the time dependence of the recovery of the amide proton signal intensity was monitored. To eliminate dynamic range problems arising from preirradiation of the water signal by the saturation pulse, a homogeneity spoiling pulse was included between the decoupler saturation pulse and the Redfield pulse. The spoiling pulse hardware and software were the same as described elsewhere (Montelione et al., 1984).

The first-order recovery ($T_{1,app}$) of the peak intensity was determined from linear least-squares fits of ln $([I(\infty) - I(\tau)]/I(\infty))$ vs. delay time (τ), where $I(\tau)$ is the peak intensity after a delay time τ and $I(\infty)$ is the peak intensity after a long delay time ($>8T_{1,app}$). The logarithmic plots were linear in every case, with a slope equal to $-1/T_{1,app}$.

Rate Determinations. The pseudo-first-order rate constants for secondary amide proton exchange in H_2O were calculated assuming the high-mobility dynamic limit, in which transitions between intramolecular hydrogen-bonded conformations and solvent hydrogen-bonded conformations are rapid relative to the rate of proton exchange (i.e., proton exchange is rate limiting). In this case, the exchange rate constant, k_{ex}, is given by

$$k_{ex} = \eta / T_{1,app} \quad (1)$$

The component of the apparent longitudinal relaxation time, $T_{1,app}$, due only to magnetic contributions, $T_{1,mag}$, is obtained simply by subtracting the exchange contribution:

$$1/T_{1,mag} = 1/T_{1,app} - k_{ex} \quad (2)$$

The observed exchange rate in water represents the sum of the acid-catalyzed, base-catalyzed, and the uncatalyzed (other) rates. In the region of pH 4–7 employed in these studies, the base-catalyzed exchange predominates in the amide proton exchange in peptides (Molday et al., 1972), and

$$k_{ex} = k_{OH}[OH^-]^n \quad (3)$$

where k_{OH} is the base-catalyzed rate constant. Simple first-order base catalysis is assumed ($n = 1$). Hydroxide ion concentrations were determined from the measured pH and an interpolated value at 300 K of log $K_w = -13.93$ (Weast, 1975), assuming unit activity coefficient for the hydroxide ion (see footnote *a* of Table II).

Errors. In the saturation-transfer experiment, the uncertainty in the measurement of a peak intensity was assumed to be 5% of the measured intensity. The uncertainty in the determination of the relaxation time was assumed to be the standard error in the slope of the linear least-squares plot. Errors were propagated in the usual manner. Those in Table II are the estimated uncertainties. The error symbols in Figure 4 correspond to the deviations for k_{ex} in Table II. The errors in k_{OH} are given in the last column of Table II.

Results

Amide Proton Assignments. The chemical shifts of the centers of the multiplets for the amide proton resonances that have been assigned are shown in Table I. These are expressed relative to 4.80 ppm for the water (HOD) resonance. It should be remembered that amide and water proton resonances tend to be broad, with chemical shifts that vary with both temperature and pH. Thus, the second decimal place is included only to demonstrate the consistency between the various peptides in both the absolute as well as relative peak positions of the individual resonances throughout the series of peptides. The 600-MHz probe lacked a facility for maintaining constant temperature. The 300-MHz measurements were made at a nominal probe temperature of 300 K.

N-Methylamide proton resonances were assigned on the basis of their quartet character and their spin–spin coupling with the methyl proton resonances. Glycine amide proton resonances were distinguished from the remaining amide proton resonances by their "triplet" appearance (actually a doubled doublet). Individual glycine amide proton assignments were made from three different preparations of F-6 in which perdeuterated glycine was incorporated at positions P_4, P_3, and P_1', respectively. The resulting amide proton singlets established the assignment and facilitated the determinations of some of the exchange rates. Peptide F-9 had perdeuterated glycine at position P_3.

Temperature Dependence of Amide Proton Chemical Shifts. The results of the temperature-dependence measurements are summarized in Figure 2. In peptide F-9, only the Gly(P_3) amide proton exhibits a temperature dependence (−6.1 ppb/deg), which is significantly smaller than those for the other amide proton resonances (−7.3 to −8.7 ppb/deg). In peptides F-6 and F-8, only the Gly(P_3) and Gly(P_4) amide protons exhibit reduced slopes (−5.9 to −6.2 ppb/deg) relative to the other amide protons in these peptides (−6.8 to −9.4 ppb/deg).

Gly(P_3) Amide Proton Exchange Rates. Figure 3 shows representative saturation-transfer experiments for peptides F-9

Table II: Gly(P_3) Amide Proton Exchange Rates at 300 K

peptide	pH	η	$T_{1,app}$ (s)	k_{ex} (s^{-1})	$T_{1,mag}$ (s)	$k_{OH} \times 10^8$ (M^{-1} s^{-1})[a]
F-9	5.02	0.27 ± 0.07	0.52 ± 0.01	0.52 ± 0.15	0.71 ± 0.09	4.4 ± 1.8
	5.02	0.28 ± 0.07	0.47 ± 0.01	0.60 ± 0.16	0.65 ± 0.09	5.1 ± 1.9
	5.23	0.48 ± 0.05	0.39 ± 0.01	1.23 ± 0.17	0.75 ± 0.13	6.6 ± 1.7
	5.49	0.63 ± 0.04	0.27 ± 0.01	2.33 ± 0.22	0.73 ± 0.19	6.3 ± 1.3
	5.85	0.74 ± 0.03	0.18 ± 0.01	4.11 ± 0.26	0.69 ± 0.27	4.4 ± 0.8
						av 5.4 (SD 1.0)
F-8	4.94	0.04 ± 0.10	0.30 ± 0.01	0.13 ± 0.32	0.31 ± 0.04	1.4 ± 3.6
	4.99	0.09 ± 0.09	0.28 ± 0.02	0.32 ± 0.35	0.31 ± 0.06	2.7 ± 3.3
	5.37	0.24 ± 0.08	0.26 ± 0.01	0.92 ± 0.33	0.34 ± 0.06	3.1 ± 1.5
	5.92	0.42 ± 0.06	0.22 ± 0.01	1.91 ± 0.32	0.38 ± 0.08	2.0 ± 0.6
	6.05	0.57 ± 0.04	0.16 ± 0.01	3.56 ± 0.43	0.37 ± 0.11	2.4 ± 0.6
						av 2.3 (SD 0.7)
F-7	5.60	0.47 ± 0.05	0.21 ± 0.01	2.24 ± 0.30	0.40 ± 0.08	4.8 ± 1.2
F-6	5.38	0.41 ± 0.06	0.27 ± 0.01	1.52 ± 0.25	0.46 ± 0.08	5.2 ± 1.4

[a] The activity coefficient of OH^- departs from unity (in the absence of salt) by at most 2% over the pH range of 4.9–6.1 (Kielland, 1937). Therefore, it was taken as unity in computing the concentration of OH^- from the measured pH.

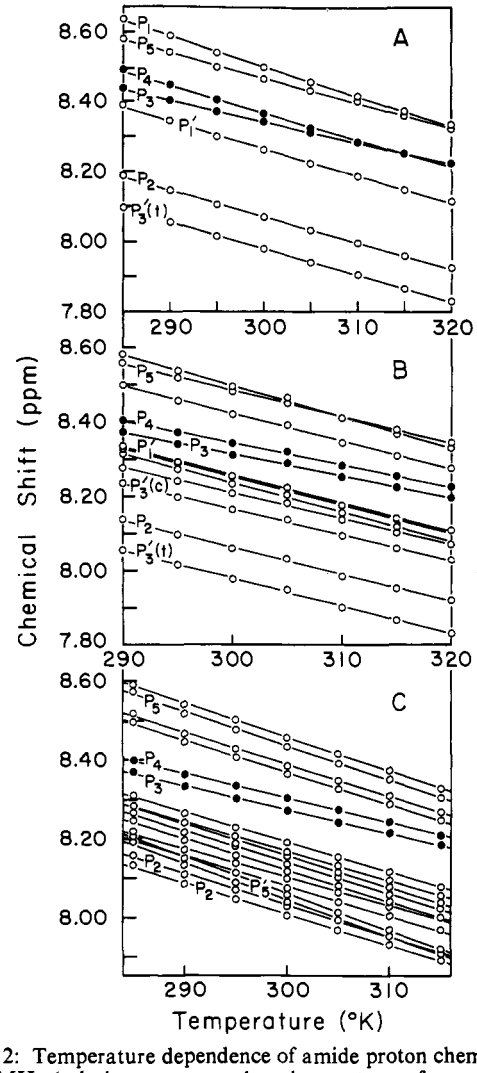

FIGURE 2: Temperature dependence of amide proton chemical shift at 300 MHz (relative to a nonexchanging proton, referenced to 4.80 ppm for the HOD resonance at 300 K) for (A) multiplet centers of F-9 at pH* 4.8, (B) multiplet centers of F-6 at pH* 4.9, and (C) *each* resolvable peak of F-8 at pH* 4.5. Solid circles pertain to the *centers* of the Gly(P_4) and Gly(P_3) multiplet (a singlet for P_3 of F-9).

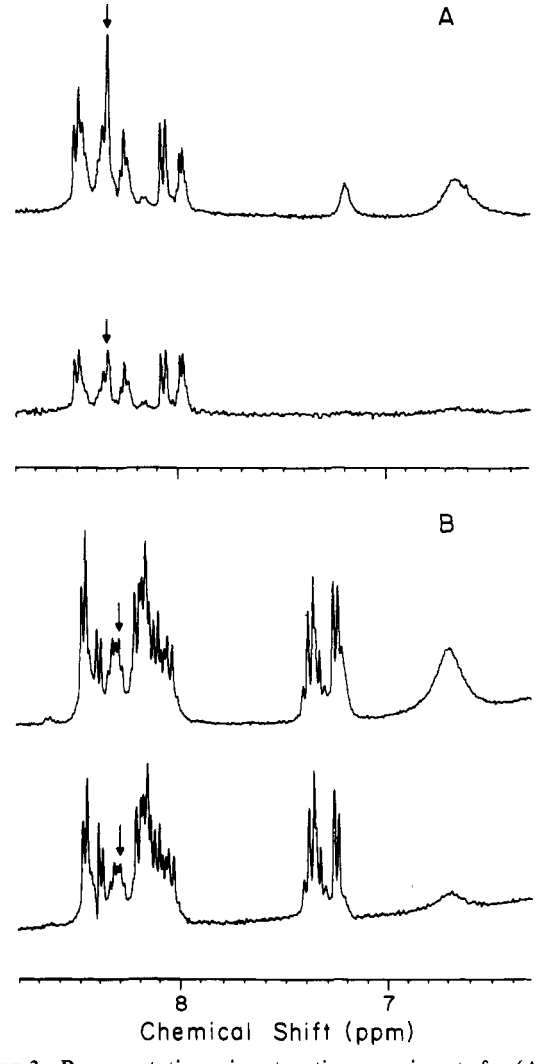

FIGURE 3: Representative spin saturation experiments for (A) F-9 and (B) F-8. Lower traces were obtained with solvent water saturation. Arrows indicate the Gly(P_3) amide proton resonance.

and F-8. Table II contains the results of the determinations of exchange rates. The values of $T_{1,mag}$ for a particular peptide were observed to be independent of pH. Figure 4 depicts the measured exchange rates for these peptides as a function of pH. The linear fits (with a slope of 1) of the data for F-9 and F-8 fall outside of the error limits for several points, suggesting that the uncertainties have been underestimated.

Discussion

Temperature Dependence of Amide Proton Chemical Shifts. The temperature dependence of amide proton chemical shifts has been used as an indicator of solvent accessibility (Kopple et al., 1969; Ohnishi & Urry, 1969; Llinas et al., 1970; Urry et al., 1975). In Me_2SO, amide protons of peptides generally exhibit slopes around −6 ppb/deg whereas those that are shielded from solvent generally exhibit much lower slopes. While the measured slopes vary from one solvent to another,

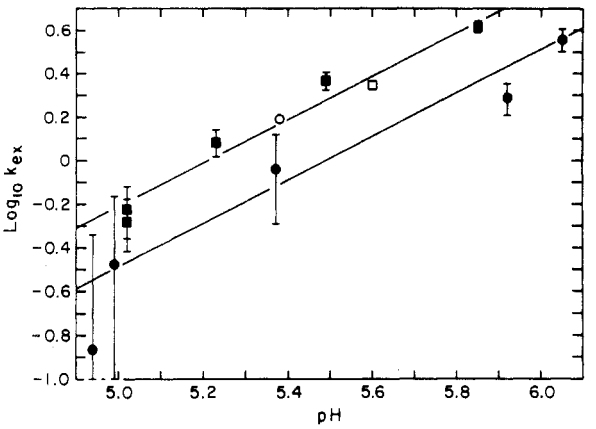

FIGURE 4: Measured exchange rate constants, k_{ex}, as a function of pH for the Gly(P_3) amide proton of (■) F-9, (●) F-8, (□) F-7, and (○) F-6. Lines represent best fit for F-9 and F-8 (excluding the value at pH 4.94) with slope of 1.

the amide protons show similar trends relative to each other. Thus, exposed amide protons exhibit larger temperature dependences than those that are hydrogen bonded in the various solvents that have been examined (Llinas & Klein, 1975). In aqueous solutions of peptides, amide proton resonances have been observed to broaden and move toward the solvent water peak when the temperature is raised, as would be expected for protons that exchange on the NMR time scale. However, neither the amide proton chemical shift nor its temperature dependence is expected to correlate simply with its exchange rate. In considering the results of the variable-temperature studies, we assume that markedly reduced temperature dependences of amide proton chemical shifts in water may reflect hydrogen bonding or shielding from solvent in a manner analogous to that observed in Me_2SO. We arbitrarily define a markedly reduced slope (ppb/deg) as one whose absolute value is less than the absolute value of the mean slope minus one standard deviation. The results of the variable-temperature studies are summarized in Figure 2. In interpreting these results, it must be emphasized that any conformational features that are responsible for a reduced slope exist in an ensemble of numerous conformational states in these linear peptides.

For F-9, only the Gly(P_3) amide proton resonance exhibits a relatively smaller (by ~22%) slope (−6.1 ppb/deg), suggesting that this amide proton may be involved in hydrogen bonding. This constitutes qualitative evidence for a conformational preference for at least some β-bend in this region, viz., at Gly(P_5)-Gly(P_4), residues $i + 1$ and $i + 2$, respectively. The fact that the temperature dependence for the Gly(P_4) amide proton is normal suggests that this proton is not shielded in peptide F-9; presumably, one or more of the residues from Phe(P_9) to Glu(P_6), not present in this peptide, are required for shielding this proton.

In F-6 and F-8, both the Gly(P_3) and the Gly(P_4) amide protons exhibit reduced temperature dependencies. No other resonances of these peptides exhibit reduced temperature dependencies. A β-bend at Gly(P_5)-Gly(P_4), residues $i + 1$ and $i + 2$, with the amide NH of Gly(P_3) involved in a hydrogen bond and with additional shielding from residues Phe(P_9) to Glu(P_6) could account for the reduced slopes. Alternatively, an equilibrium mixture involving several different bends is also consistent with the participation of Gly(P_3) and Gly(P_4) in hydrogen bonding. Such a mixture could include the proposed bend at Gly(P_5)-Gly(P_4) as well as bends at Gly(P_4)-Gly(P_3) and at Glu(P_6)-Gly(P_5). These possible bend structures are represented schematically in Figure 5.

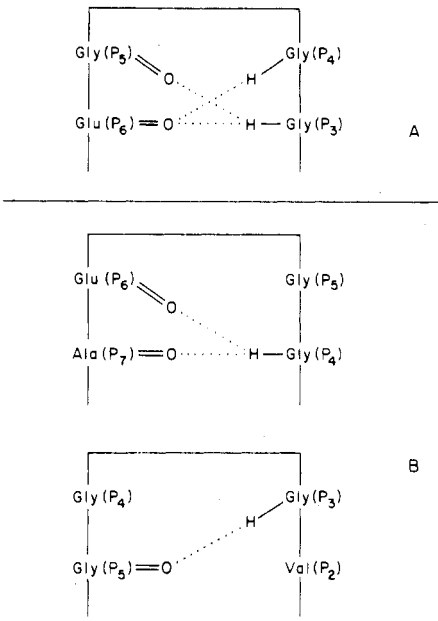

FIGURE 5: Hydrogen-bonding schemes and bends that are consistent with the variable-temperature data. A single bend as in (A) could account for the reduced slopes of the temperature dependence of the chemical shift of both the Gly(P_4) and Gly(P_3) amide protons but may also contain contributions from other bends as in (B). Alternatively, amide protons that are shielded from solvent (presumably by a β-bend) but lack hydrogen bonds could also account for the data.

The variable-temperature studies provide qualitative evidence for the existence of the proposed bend structures in aqueous solution. From these data, however, it is not possible to estimate the equilibrium distribution between the intramolecular hydrogen-bonded and solvent-bonded amides or to assess the relative tendency to form hydrogen-bonded structures (β-bends) among the various peptides. Finally, the reduced temperature dependencies may actually arise from shielding of these protons from solvent water rather than hydrogen-bond formation, although such shielding would also likely reflect a conformational feature such as a β-bend.

Saturation Transfer and Base-Catalyzed Exchange Rate Constant. In an effort to assess the relative tendencies of these peptides to form hydrogen bonds (or β-bends), saturation-transfer experiments were used to determine the Gly(P_3) amide proton exchange rate in each of the peptides. The mean base-catalyzed exchange rate constant, k_{OH}, for the Gly(P_3) amide proton of F-9 is 5.4×10^8 M^{-1} s^{-1}; the mean k_{OH} for the same amide proton in F-8 is 2.3×10^8 M^{-1} s^{-1}. We propose that this 2-fold reduction in the base-catalyzed amide proton exchange rate constant reflects a slightly greater tendency for this amide proton to be hydrogen bonded or shielded from solvent in F-8 relative to F-9. It should be emphasized that the magnitude of this effect, although significant, is still quite small. Llinas et al. (1973), Philson & Bothner-By (1979), Krauss & Chan (1982), and Narutis & Kopple (1983), all studying cyclic peptides, observed much larger reductions in the base-catalyzed exchange rate constants from those predicted by the linear free-energy relation proposed by Molday et al. (1972), some even greater than 3000-fold. The limited conformational space available to these cyclic peptides results in significant populations of a limited number of low-energy conformations that can shield amide protons or stabilize hydrogen bonds. Such a large effect on the exchange rate constant is neither expected nor observed for short linear peptides such as those studied here because of the large number of conformational states in the ensemble.

As can be seen in Table II, the values of k_{OH} of 4.8×10^8

and 5.2×10^8 M^{-1} s^{-1} determined at a single pH for F-7 and F-6, respectively, are similar to the values obtained for F-9. This is consistent with our proposal that the small but significant difference in the value of k_{OH} for F-8, compared to those of the other peptides, F-9, F-7, and F-6, reflects a greater tendency for F-8 to form a β-bend in the Gly(P_3) region thereby reducing exchange rate constants because of reduced solvent accessibility and/or hydrogen-bond formation. While other explanations can account for these observations, a greater tendency for F-8 to form β-bends is supported by previous kinetic studies described in the introduction. A β-bend at Gly(P_5)-Gly(P_4) with the rest of F-8 in an extended chain conformation could bring Asp(P_{10}) and Arg(P_3') into close spatial proximity. The formation of a salt link between these two residues would serve to stabilize the β-bend, resulting in a smaller Gly(P_3) amide proton exchange rate constant. A diagram showing a β-bend at Gly(P_4)-Gly(P_3) and the proposed salt link was presented in Figure 4 of Marsh et al. (1983); with the data reported here, the same diagram is applicable except that the bend should be shifted to Gly-(P_5)-Gly(P_4), thereby bringing the required Phe(P_9) even closer to the Arg(P_1)–Gly(P_1') peptide bond.

The temperature dependencies of the amide proton chemical shifts suggest that the Gly(P_3) amide proton is either hydrogen bonded or shielded from solvent in all of the peptides studied. This suggests that there is a tendency toward formation of a β-bend in all of these peptides. The 2-fold smaller exchange rate constant for the P_3 amide proton in F-8 relative to all of the other peptides (F-6, F-7, and F-9) suggests that the conformational features (i.e., β-bend) responsible for the lowered temperature dependence are somehow further stabilized in the F-8 peptide. To account for the enhanced rate of hydrolysis of the Arg(P_1)–Gly(P_1') peptide bond of F-8 by thrombin, it was proposed earlier (Marsh et al., 1983) that a salt link between the side chains of Asp(P_{10}) and Arg(P_3') stabilizes a bend in the intervening region near Gly(P_3). These NMR studies provide more direct evidence for the proposed β-bend and additional indirect evidence for the proposed salt link.

Other evidence supports the possible existence of a β-bend in this portion of the Aα chain. Hanna et al. (1984) showed that phosphorylation of Ser(P_{14}) increases the rate of release of fibrinopeptide A from human fibrinogen due to enhanced binding of thrombin, and experiments of Kudryk et al. (1982) suggest that newly secreted (dog) fibrinogen is almost entirely in its phosphorylated form. Thus, a salt link between the phosphate group on Ser(P_{14}) and the side chain of Arg(P_7'), in addition to the proposed one between Asp(P_{10}) and Arg(P_3'), could exist (and enhance thrombin action) if this portion of the Aα chain adopted the β-bend conformation. The presence of such a β-bend would also bring the P_1'–P_4' portion of the chain close to the P_{10}–P_{15} portion; in fact, such an interaction, but a *bimolecular* one (between the P_{10}–P_{15} portion of fibrinopeptide A and the tetrapeptide Gly-Pro-Arg-Pro, a P_1'–P_4' analogue), has recently been demonstrated by NMR measurements (Root-Bernstein & Westall, 1984).

It is of interest to note that the sequence -Gly-Gly-Gly- appears in the Aα chain of the fibrinogens of almost all animal species in positions corresponding to P_5-P_4-P_3 (Dayhoff, 1972). This suggests that the -Gly-Gly-Gly- tripeptide may serve a structure/function role in accommodating a β-bend in this portion of the Aα chain.

ACKNOWLEDGMENTS

We thank T. W. Thannhauser for carrying out the amino acid analyses, G. T. Montelione for help with the experimental work, E. R. Stimson for helpful comments on the manuscript, and both G. T. Montelione and E. R. Stimson for many helpful discussions.

SUPPLEMENTARY MATERIAL AVAILABLE

Detailed experimental procedure and properties of the intermediates (5 pages). Ordering information is given on any current masthead page.

Registry No. I, 96055-71-9; II, 96055-72-0; III, 96055-73-1; IV, 96055-74-2; V, 96095-14-6; VI, 96055-75-3; VII, 96055-76-4; VIII, 96055-70-8; F-6, 74360-78-4; F-7, 83268-85-3; F-8, 86177-72-2; F-9, 96055-69-5; H-Gly-OH, 56-40-6; Z-Gly-OH, 1138-80-3; H-Pro-$NHCH_3$, 52060-82-9; BOC-Arg(NO_2)-OH, 2188-18-3; BOC-Val-OH, 13734-41-3; Z-Gly-OSu, 2899-60-7; Z-Gly-Gly-OH, 2566-19-0; thrombin, 9002-04-4.

REFERENCES

Blombäck, B. (1967) in *Blood Clotting Enzymology* (Seegers, W. H., Ed.) pp 143–215, Academic Press, New York.

Campbell, I. D., Dobson, C. M., & Ratcliffe, R. G. (1977) *J. Magn. Reson. 27*, 455.

Campbell, I. D., Dobson, C. M., Ratcliffe, R. G., & Williams, R. J. P. (1978) *J. Magn. Reson. 29*, 397.

Claeson, G., Aurell, L., Karlsson, G., & Friberger, P. (1977) in *Proceedings of the Symposium of the Deutsche Gesellschaftfuer Klinische Chemie*, Titisee, Breisgau, Germany, July 1976 (Witt, I., Ed.) pp 37–54, de Gruyter, Berlin and New York.

Dayhoff, M. O. (1972) in *Atlas of Protein Sequence and Structure*, Vol. 5, p D-90, National Biomedical Research Foundation, Silver Spring, MD.

Dayhoff, M. O. (1973) in *Atlas of Protein Sequence and Structure*, Supplement 1, pp S-29, S-87, National Biomedical Research Foundation, Silver Spring, MD.

Dayhoff, M. O. (1976) in *Atlas of Protein Sequence and Structure*, Supplement 2, p 257, National Biomedical Research Foundation, Silver Spring, MD.

Hanna, L. S., Scheraga, H. A., Francis, C. W., & Marder, V. J. (1984) *Biochemistry 23*, 4681.

Henschen, A., Southan, C., Kehl, M., & Lottspeich, F. (1981) *Thromb. Haemostasis 46*, 181 (Abstr. 559).

Kielland, J. (1937) *J. Am. Chem. Soc. 59*, 1675.

Kopple, K. D., Ohnishi, M., & Go, A. (1969) *Biochemistry 8*, 4087.

Krauss, E. M., & Chan, S. I. (1982) *J. Am. Chem. Soc. 104*, 6953.

Krishna, N. R., Huang, D. H., Glickson, J. D., Rowan, R., III, & Walter, R. (1979) *Biophys. J. 26*, 345.

Krishna, N. R., Goldstein, G., & Glickson, J. D. (1980) *Biopolymers 19*, 2003.

Kudryk, B., Okada, M., Redman, C. M., & Blombäck, B. (1982) *Eur. J. Biochem. 125*, 673.

Llinas, M., & Klein, M. P. (1975) *J. Am. Chem. Soc. 97*, 4731.

Llinas, M., Klein, M. P., & Neilands, J. B. (1970) *J. Mol. Biol. 52*, 399.

Llinas, M., Klein, M. P., & Neilands, J. B. (1973) *J. Biol. Chem. 248*, 915.

Marsh, H. C., Jr., Meinwald, Y. C., Lee, S., & Scheraga, H. A. (1982) *Biochemistry 21*, 6167.

Marsh, H. C., Jr., Meinwald, Y. C., Thannhauser, T. W., & Scheraga, H. A. (1983) *Biochemistry 22*, 4170.

Meinwald, Y. C., Martinelli, R. A., Van Nispen, J. W., & Scheraga, H. A. (1980) *Biochemistry 19*, 3820.

Molday, R. S., Englander, S. W., & Kallen, R. G. (1972) *Biochemistry 11*, 150.

Montelione, G. T., Arnold, E., Meinwald, Y. C., Stimson, E. R., Denton, J. B., Huang, S. G., Clardy, J., & Scheraga,

H. A. (1984) *J. Am. Chem. Soc. 106*, 7946.
Morris, S., Denninger, M. H., Finlayson, J. S., & Menache, D. (1981) *Thromb. Haemostasis 46*, 104 (Abstr. 315).
Nagy, J. A., Meinwald, Y. C., & Scheraga, H. A. (1982) *Biochemistry 21*, 1794.
Narutis, V. P., & Kopple, K. D. (1983) *Biochemistry 22*, 6233.
Ohnishi, M., & Urry, D. W. (1969) *Biochem. Biophys. Res. Commun. 36*, 194.
Philson, S. B., & Bothner-By, A. A. (1979) *Proceedings of the American Peptide Symposium, 6th* (Gross, E., & Meienhofer, J., Eds.) pp 219–222, Pierce Chemical Co., Rockford, IL.
Rae, I. D., & Scheraga, H. A. (1979) *Int. J. Pept. Protein Res. 13*, 304.
Redfield, A. G., Kunz, S. D., & Ralph, E. K. (1975) *J. Magn. Reson. 19*, 114.
Root-Bernstein, R. S., & Westall, F. C. (1984) *Proc. Natl. Acad. Sci. U.S.A. 81*, 4339.
Schecter, I., & Berger, A. (1967) *Biochem. Biophys. Res. Commun. 27*, 157.
Urry, D. W., Long, M. M., Mitchell, L. W., & Okamoto, K. (1975) in *Peptides: Chemistry, Structure and Biology* (Walter, R., & Meienhofer, J., Eds.) p 113, Ann Arbor Science, Ann Arbor, MI.
Van Nispen, J. W., Hageman, T. C., & Scheraga, H. A. (1977) *Arch. Biochem. Biophys. 182*, 227.
Weast, R. C. (1975) *Handbook of Chemistry and Physics*, p D-152, CRC Press, Cleveland, OH.

Large-Scale Purification, Oligomerization Equilibria, and Specific Interaction of the LexA Repressor of *Escherichia coli*†

M. Schnarr,* J. Pouyet, M. Granger-Schnarr, and M. Daune

Laboratoire de Biophysique, Institut de Biologie Moléculaire et Cellulaire du CNRS, 67084 Strasbourg Cedex, France

Received July 27, 1984

ABSTRACT: A rapid large-scale procedure for the purification of the LexA repressor of *Escherichia coli* is described. This procedure allows one to get more than 100 mg of purified protein from 100 g of bacterial paste with a purity of at least 97%. This method is comparable to earlier, far more complicated purification procedures giving clearly smaller yields. It is shown that the LexA protein may be identified spectroscopically by a large A_{235}/A_{280} ratio and very pronounced ripples in the absorption spectrum arising from a high amount of phenylalanine residues with respect to that of the other aromatic amino acids. Polyacrylamide gel electrophoresis has been used to study the specific interaction of LexA with a recA operator fragment. The quaternary structure of LexA has been studied by equilibrium ultracentrifugation and sedimentation velocity measurements. The sedimentation coefficient increases with increasing LexA concentration, indicating that LexA is involved in self-association. This finding has been confirmed by equilibrium ultracentrifugation. The results are best described by a monomer–dimer and a subsequent dimer–tetramer equilibrium, with an association constant of 2.1×10^4 M^{-1} for the dimer and 7.7×10^4 M^{-1} for the tetramer formation. These relatively small association constants determined under near-physiological pH and salt conditions suggest that in vivo LexA should be essentially in the monomeric state. The degree to which LexA decreases the electrophoretic mobility of a 175 base pair fragment harboring the recA operator suggests that the recA operator interacts nevertheless with a LexA dimer. However, our results may be also explained by the binding of a LexA monomer with a simultaneous bending of the DNA fragment.

Exposure of *Escherichia coli* to agents or conditions that either damage DNA or interfere with DNA replication results in the increased expression of genes that are members of the SOS regulatory system [for reviews see Witkin (1976), Little & Mount (1982), and Walker (1984)]. During normal cell growth this set of unlinked genes is repressed by the LexA protein. Upon DNA damage an inducing signal is generated that activates the RecA protein. This activated form of RecA stimulates the specific cleavage of lexA gene product (LexA)[1] at an alanine–glycine bond near the center of the protein, leading to an inactivation of LexA and the derepression of the SOS genes. At elevated pH values the same peptide bond is cleaved in the absence of RecA, suggesting that the inactivation of LexA may proceed via autodigestion (Little, 1984). Under in vivo conditions activated RecA protein is necessary to stimulate this reaction, leading to a complete degradation of LexA within a few minutes (Little, 1983). In contrast to the cleavage of λ repressor (Phizicky & Roberts, 1980; Cohen et al., 1981; Little, 1984) the cleavage of LexA seems to be independent of the repressor concentration (Little, 1984). It has been concluded from these results that in the case of λ repressor only the monomer is susceptible to cleavage whereas the LexA protein can be cleaved as well as if it is a monomer or part of a dimer (Little, 1984).

Here, we show by sedimentation equilibrium and velocity measurements that under near-physiological pH and salt

† This work was supported in part by Grant 81.E.1225 of the former Délégation Générale à la Recherche Scientifique et Technique.

[1] Abbreviations: LexA, lexA gene product; IPTG, isopropyl β-D-thiogalactoside; Tris, tris(hydroxymethyl)aminomethane; EDTA, ethylenediaminetetraacetic acid; ME, 2-mercaptoethanol; DTT, dithiothreitol; CAP, catabolite gene activator protein; bp, base pair; SDS, sodium dodecyl sulfate.

0006-2960/85/0424-2812$01.50/0